DESIGN OF AROMATIC THERMOSETTING POLYESTER COMPOSITES FOR THERMALLY STABLE DEVICES

BY

MENGXI GUO

THESIS

Submitted in partial fulfillment of the requirements
for the degree of Master of Science in Materials Science and Engineering
in the Graduate College of the
University of Illinois at Urbana-Champaign, 2014

Urbana, Illinois

Adviser:

Professor James Economy

ABSTRACT

Aromatic thermosetting copolyester (ATSP) has been under development since 1995 in Professor James Economy's research group at the University of Illinois, Urbana-Champaign. It can be seen as a major development in high performance polymers as it affords a highly processable series of routes towards diverse form factors that may need to utilize a highly thermally resistant (and therefore all-aromatic) thermosetting polymer. Prior and current study has demonstrated its outstanding thermal stability and resistance to flame, capability of ablation and high wear resistance. It shows strong bonding with fibers and thus ATSP can be used as resin matrix in polymer/fiber composites. ATSP is soluble in a number of polar aprotic solvents and can be in this regard used as an effective tribological and corrosion coating for metal components.

The two-step synthesis of the ATSP is an effective and smooth synthesis that affords an immense range of tailorability both in terms of cross-link density and constituent monomers. In this thesis, firstly, new aromatic monomers, such as resorcinol diacetate and 3, 5-diacctoxybenzoic acid, are employed in the synthesis of ATSP oligomers. These have the effect of reducing condensation reaction temperature and the viscosity of the oligomer and its solutions. In the thesis, firstly, several new aromatic monomers are added to the ATSP synthesis. The condensation reaction temperature reduces and the viscosity of the oligomer solution significantly drops. Secondly, H^1-NMR is introduced into the characterization. Average molecular weight of each batch of oligomers can be calculated by a simple relationship. Origins of liquid crystalline feature are discussed and more oligomers are synthesized.

After reviewing the work on ATSP/carbon fiber composites, ATSP/glass fiber composite was fabricated. The thickness of the composite laminate can be easily controlled by bonding cured thin laminate together in a solid-state manner. The interlaminar shear strength of ATSP/glass fiber is measured by single fiber fragmentation test. Fiber induced local orientation of ATSP is observed. ITR process is proved to be effective in repairing the cracks and scratches of composites. In addition, the first electrical property test is achieved on ATSP/glass fiber composite. The insertion loss is less than standard circuit board FR-4.

ACKNOWLEDGMENTS

Studying at University of Illinois and working with Prof. Economy's group has been a valuable experience. First, I would like to thank my advisor, Prof James Economy. With his support, guidance and understanding, I was able to finish my work on ATSP composites. His dedication for developing improved materials always motivated me. Next, I would like to thank my research partner, Jacob Meyer, who has helped me design and perform the experiments during the past three years. He has shared many helpful conversations with me from using lab equipment to the understanding of polymers and fibers. He provided many creative research ideas and he is devoted to the ATSP projects. And then I would like to thank my group mates: Weihua Zheng, James Langer, Yaxuan Yao and Shanshan Zhao. They have been supporting me and sharing valuable academic experiences with me. The group has always been a pleasure in the working place. Next, I would like to thank Dr. Dean Olson who introduced the NMR lab to me and trained me to perform NMR tests. Next, I would like to thank my parents for their nurturing love and continuous support. Last but not least, I would like to thank all my friends at Champaign-Urbana for the joyful days we have had together.

TABLE OF CONTENTS

LIST OF FIGURES

LIST OF TABLES

CHAPTER 1

INTRODUCTION

1.1 Printed Circuit Boards

Printed circuit boards (PCB) are widely used today as the substrate for electronic components. It is usually formed by a thin layer of conductive material, which is deposited onto an insulating laminate. The board can be single-sided, double sided or multilayer. Multilayer boards are made of several double sided boards glued together with small conductive holes connecting each layer. It is applied to high density electronic components. [1]

The polymer composites materials are the most commonly used system for the laminate. The composites are formed by the use of high performance resin matrix as adhesive and the reinforcement as support. The polymer resin types vary from epoxies to polyesters, polyimide to polyphenylene oxide and PTFE. [1] To choose from these high performance resins, several properties should be considered, like processability, flammability, chemical resistance, electrical properties and thermal stability. Among these materials, epoxy is the most commercially successful resin because of its relative low processing temperature, low cost, and ease of use. Epoxy is the term used for the cured thermosetting product from polymers with epoxide end groups.

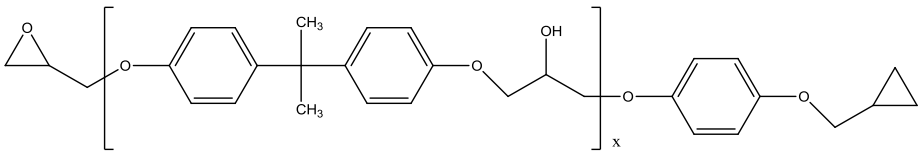

Figure 1.1: Reactive oligomer with epoxide group

The reinforcements used in the laminates are generally glass fabrics, like woven glass fiber or glass fiber paper. It has a relative high dielectric constant, an excellent tensile strength and rigidity. One of the most commercially used printed circuit boards is FR-4 which is made of epoxy/glass fiber. The typical engineering values are listed. [1]

Table 1.1: Properties of FR-4. From Plastics International data sheet [2]

Property	Unit	Epoxy/Glass Fiber FR-4
Moisture Absorption	%	0.15
Rockwell Hardness	M scale	110
Tensile Strength (LW)	psi	4500
Izod Impact Strength (LW)	ft-lb/in	14.0
Compressive Strength flatwise	psi	5500
Shear Strength	psi	2200
Young's Modulus	psi	3.5×10^6
Dielectric Constant	-	4.80
Dissipation factor	-	0.025
Maximum Operating Temperature	^oC	140
Coefficient of Thernal Expansion, x-axis	ppm/^oC	15
Coefficient of Thernal Expansion, y-axis	ppm/^oC	18

There are major problems with the FR-4 in spite of its success. The laminate has poor flame resistance. It would require halogen additives as flame retardant, for example tetrabromobisphenol-A, which reacts with the epoxide and is integrated into the matrix of the resin. [3] Tetrabromobisphenol-A releases brominated compounds which act as scavengers for radicals in the flame and thus interrupt the combustion. [4] The FR-4

laminate would pick up water during the moisture environment. In addition, due to the mismatch of coefficient of thermal expansion (CTE) between epoxy and glass fiber, the laminate would suffer the residual stress at the interface and it would lead to microfractures inside the laminate during the temperature change of the environment.

Many other polymers have been tested as the resin for printed circuit board laminate. For example, high-temperature multifunctional epoxy can improve the chemical and moisture resistance. The stiffness and thermal resistance is increased because of the higher cross-link density. Another suitable resin is polyimide. It has high melting point and good chemical resistance. It is used for high temperature burn-in applications and down-hole environment since it has excellent thermal resistance. [1, 5]

1.2 Aromatic Thermosetting Polyesters (ATSP)

Since early 1990's, Professor Economy's group started the development of a cured aromatic thermosetting polyester system. [6] This work had its origins in the synthesis of the homopolymer of p-hydroxybenzoic acid by Professor Economy at the Carborundum Corporation in the early 60s. [7, 8] The polymer is synthesized from two kinds of different oligomers, one ended with a carboxylic acid group and the other one ended with an acetoxy group. Oligomers are synthesized from monomers that possess either acetoxy or carboxylic acid functional end groups (or both). This includes but is not limited to: 4-acetroxybenzoic acid, hydroquinone diacetate, isophthalic acid and trimesic acid as the crosslinker. Prior work has demonstrated that mechanical and thermal properties of ATSP resins can be tailored by the choice of monomers and the reaction molar ratio. [9, 10]

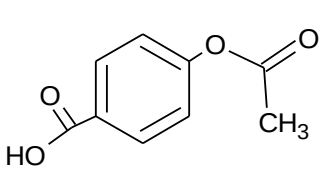

4-acetoxy-benzoic acid
(ABA)

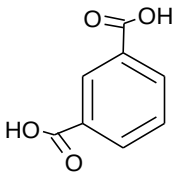

Isophthalic acid
(IPA)

Figure 1.2: Chemical structures of monomers

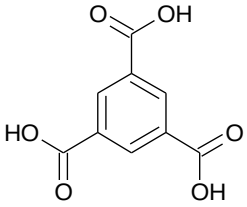

Trimesic acid
(TMA)

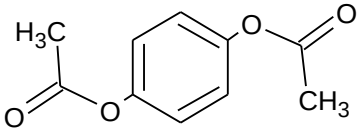

Hydroquinone diacetate
(HQDA)

Figure 1.3: Chemical structures of monomers

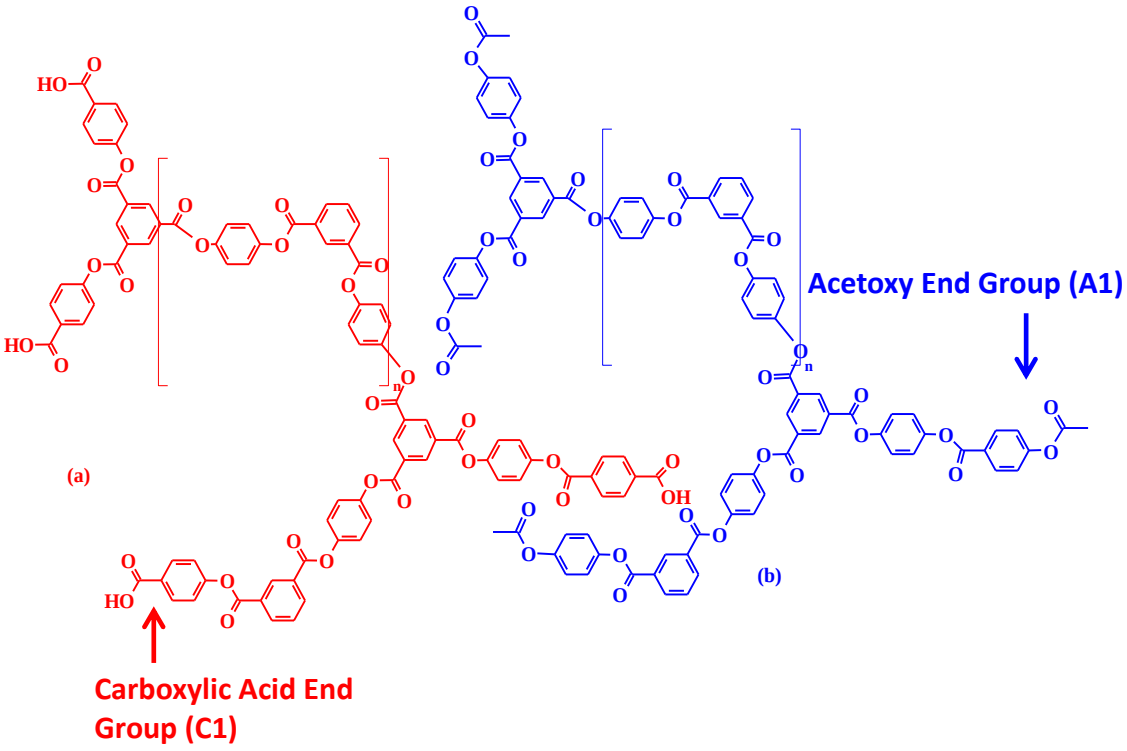

Figure 1.4: Proposed structure of ATSP

The cured ATSP can undergo interchain transesterification (ITR) reaction at high temperature. The neighboring ester bonds can be rearranged even after the polymer is fully cured. The reaction proceeds quickly at high temperature. ITR allows the resin to be repaired after mechanical fracture within the resin as well as affording a technique for solid-state bonding between fully cured components. [9, 12] The proposed mechanism of ITR is classified into three types. [11]

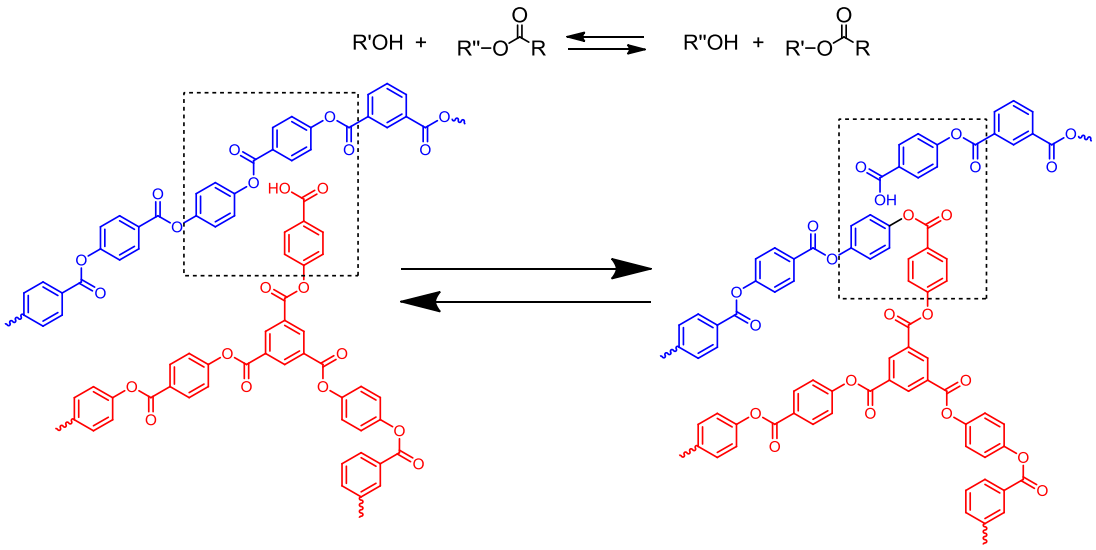

Figure 1.5: Schematic ITR process

Type 1: reaction between acetoxy end group –OAc and carboxylic acid end group –COOH. Acetic acid as byproduct is released and a chain crosslinkage is created.

Type 2: reaction between aromatic ester group and –OAc, or –COOH. It is thermodynamically favored if the monomers or dimers byproduct are volatile.

Type 3: reaction between two aromatic ester groups. No small molecular weight byproduct is given off and the reaction is in dynamic equilibrium.

ATSP shows high thermal stability because of the rigid aromatic units. It can stand up to 350 ^{o}C in air and 425 ^{o}C in nitrogen. The Tg of ATSP is as high ~285 ^{o}C. ATSP has a limiting oxygen index (LOI) value of 0.4, compared to 0.24 for epoxy.

Certain types of ATSP oligomers show liquid crystallinity behavior. They can be used to form stronger bonded composites with increased orientation. Mechanical properties can be controlled by incorporating a higher degree of chain orientation. [9, 10, 13, 14]

The potential applications of ATSP are diverse and numerous. It can be used as high temperature resin matrix with carbon fiber or glass fiber composites for re-entry spaceship coating, circuit boards, aircraft frame structure. Compared to traditional metal frame, the light weight composites is more durable due to improved fatigue resistance and low vulnerability to corrosion. It can form thick composites laminates as the multilayer circuit board substrate because of the strong interlaminar adhesion. ATSP is a suitable material for metal spray coating. It exhibits recoverable elastic deformation in instrumented scratch tests, along with outstanding wear resistance in micro-tribological experiments. ATSP coating has higher elastic recovery and thus better frictional behavior compared to PEEK coatings. [14, 15, 16]

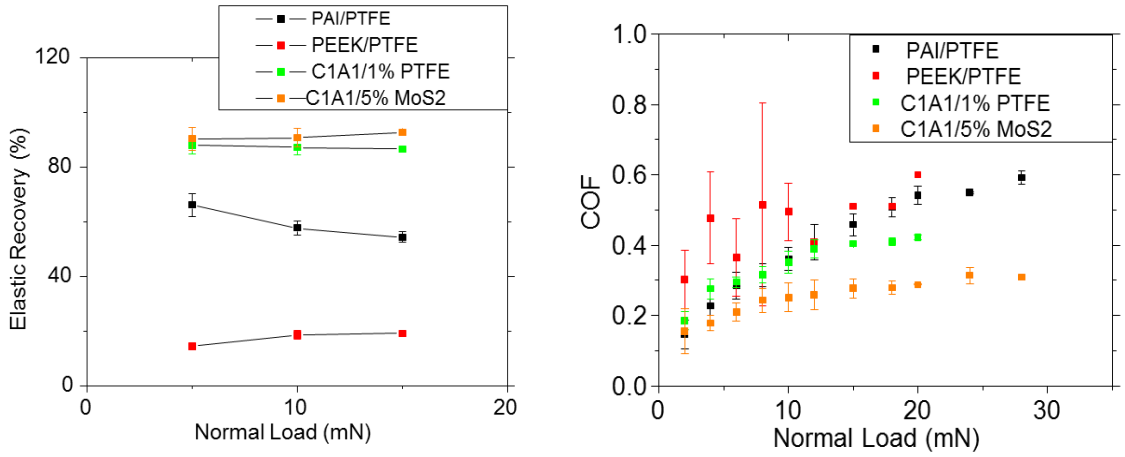

Figure 1.6: *In-situ* elastic recovery and coefficient of friction of 4 different polymeric coating surfaces. From Dr. Yeo PhD thesis [15]

1.3 Nuclear Magnetic Resonance Spectroscopy (NMR)

Over the past few decades, NMR has become an indispensable and reliable technique for determining the chemical structure of organic compounds and studying their dynamics. When an atom is in an external magnetic field, the nuclei would align with or against the direction of the magnetic field. The shift between the two states leads to a fluctuation of the magnetic field, whose frequency can be measured as chemical shift. The local atoms and geometry have a shielding effect on the magnetic field of the spin nuclei and in turn the chemical structure can be revealed by the chemical shift. NMR has been applied to characterize the molecular weight, the reactivity and the polymer stereochemistry. The molecular weight of linear polymers can be calculated by simple backbone to end group ratio relationship. Comparing the NMR results before and after a reaction can prove the formation of new bonding. For example, ^{1}H-NMR and ^{13}C-NMR are applied in analyzing the structure of a multi-component copolyester as a function of

reaction time. By quantifying the signals of chemical shift, results lead to the discussion of possible tranesterification mechanism and the statistical modeling of the average chain length. [17] Another example is that H-NMR is employed to calculate the degree of polymerization in the synthesis of poly (ester-amide)s by comparing the theoretical ester/amide molar ratio of polymer to experimental one acquired from NMR spectrum. [18] Here we use NMR spectroscopy to similarly reveal the composition and chemical structure of the synthesized aromatic polyester oligomers.

CHAPTER 2

SYNTHESIS OF LOW MELTING POINT ATSP OLIGOMERS AND CHARACTERIZATION

2.1 Backgrounds

ATSP oligomers are formed by melt condensation of several monomer units. The end functional group of oligomers is controlled by the reaction ratio. The synthesis of the ATSP oligomers was worked on by Dr. Frich. A list of various oligomers were synthesized and characterized. C-x represents the carboxylic acid terminated oligomers; and the A-x represents the acetoxy terminated oligomers. [6,10]

oligo-mer	molar feed ratio of monomer					MW_{av} (g/mol)	function-ality	softening point (°C)
	TM	TAB	ABA	IPA	HQDA			
C-1	2		6	3	4	1934	4	172
C-2*	1		6	4	4	1890	3	143
C-3	2		4	2	3	1454	4	189
C-4	2		5	1	2	1334	4	188
C-5*	1		5	2	2	1290	3	161
C-6	2		3	1	2	1094	4	162
C-7	2		3		1	854	4	148
C-8	1		3	1	1	810	3	136
A-1	2		2	2	7	1750	4	128
A-2*	1		5	2	5	1692	3	130
A-3*	1		5	1	4	1452	3	160
A-4		2	4	2	1	1270	4	128
A-5		2	2	2	1	1030	4	107
A-6		2	3	1		910	4	105
A-7		1	2	1	1	732	3	81

Figure 2.1: Oligomers data sheet. From Dr. Frich PhD thesis

The functionality of oligomers equals the difference between the total number of acetoxy groups and the total number of carboxylic acid groups in monomers. It determines the crosslinking density of the polymer.

The synthesis of functional oligomers is straight forward. Blends of acetoxy and carboxylic acid monomers were added into the reaction flask, which was purged with an argon or nitrogen gas to maintain an inert environment. After the blend was heated to 260 ℃, the loaded monomers formed a melt and acetic acid was evolved as the reaction byproduct. The acetic acid was allowed to reflux within the reaction vessel. The reflux stage was held for 30 minutes and then acetic acid was allowed to distill, affording an increase in molecular weight. Refluxing of acetic acid also allowed clearing of sublimated monomer from the reaction flask. The condenser was then reoriented to permit acetic acid to distill off. During this stage the oligomer was allowed to proceed towards theoretical (Figure 2.1) molecular weight. The acetic acid was collected and weighed in situ to provide a determination of present extent of reaction. When acetic acid production is observed to cease both by visual cue (condensation on the glass of the reaction vessel) and constant mass being observed on the weighing balance, the reaction was halted (by removal of heat flux such that the vessel returned to room temperature). The reaction melt was poured out and weighed. The melt was ground into a powder after it cooled down to room temperature. The oligomer powder was purified by Soxhlet extractor using 3:1 methanol - water solution and then dried overnight. This procedure was applied to all the oligomer synthesis through all differences in constituent monomer and monomer feed ratio.

The extent of reaction equals the ratio of collected acetic acid weight to theoretical weight. The weight difference between the reactant and the schematic oligomer product (Figure 2.2, Figure 2.3) is the theoretical weight of acetic acid as byproduct.

ATSP oligomers are dissolved in warm (around 70 ^{o}C) N-methyl-2-pyrrolidone (NMP) in various ratios and then used for making polymer/fiber composites or spray coating. Because of the high viscosity of the solution and the high melting point of the oligomers, the ATSP oligomer solutions are difficult to make. The processability of ATSP oligomers is capable of being improved by reducing the melting point of the oligomers.

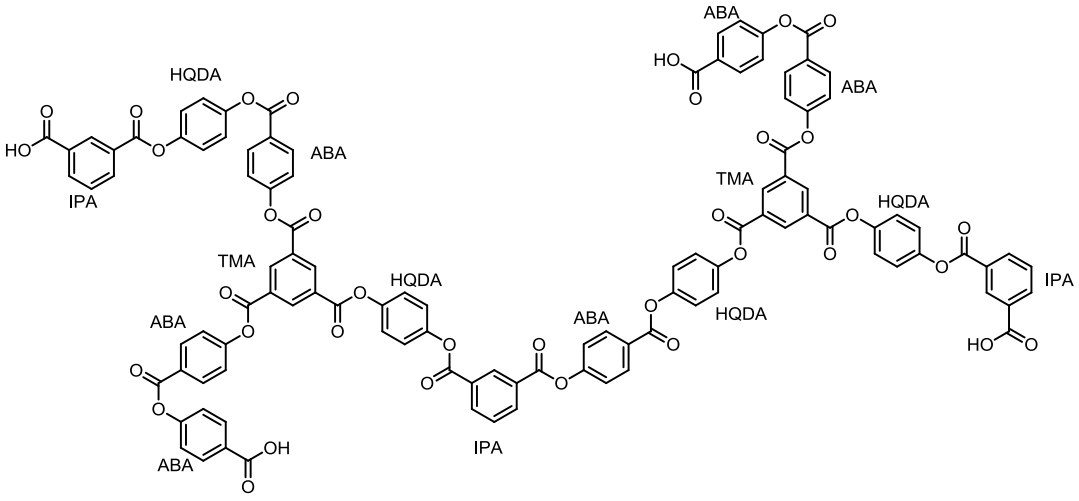

Figure 2.2: Schematic structure of C1

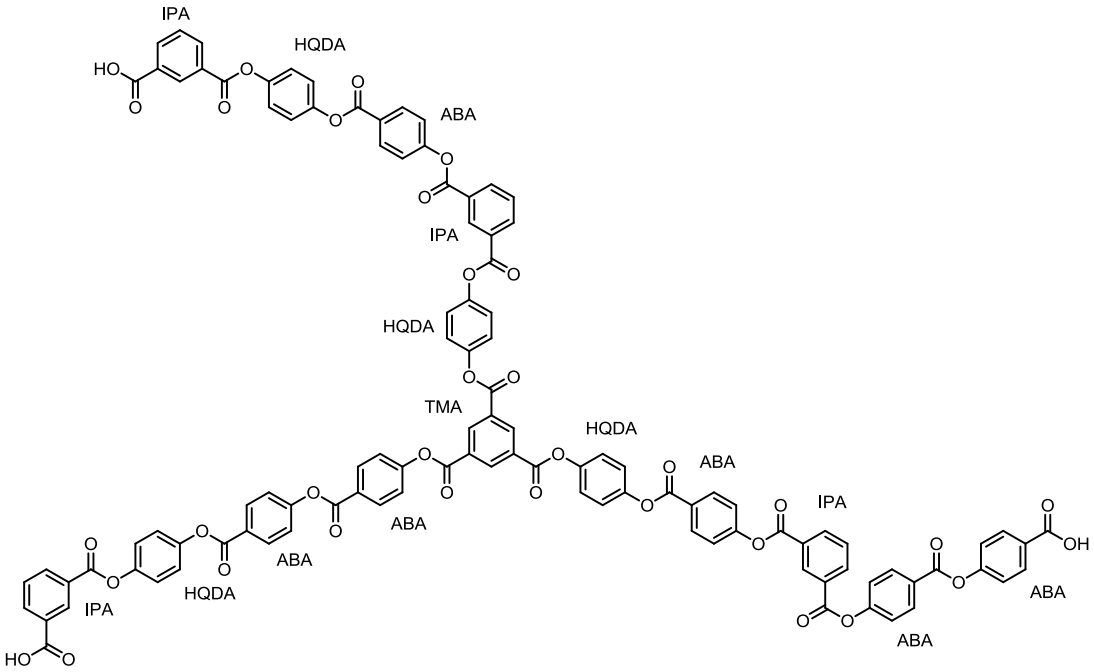

Figure 2.3: Schematic structure of C2

2.2 Synthesis of Low Melting Point ATSP Oligomers

2.2.1 RDA Based Oligomers

1, 3-phenylene diacetate (resorcinol diacetate, RDA) was chosen to substitute one of the monomers, 1, 4-phenylene diacetate (hydroquinone diacetate, HQDA). These two molecules have same molecular weight and number of functional groups. However, RDA is meta-substituted and HQDA is para-substituted, which lead to a huge difference in melting point. HQDA has a melting point around 120 ^{o}C, while RDA is a liquid at room temperature. Therefore using RDA as monomer could reduce the reaction time since the liquid phase could transfer heat more uniformly. It can also avoid the sublimation of HQDA.

3:1 TMA-RDA oligomer and 1:2 IPA-RDA oligomer is synthesized following the similar procedure as Dr. Frich used. The reaction temperature is controlled under 200 ^{o}C.

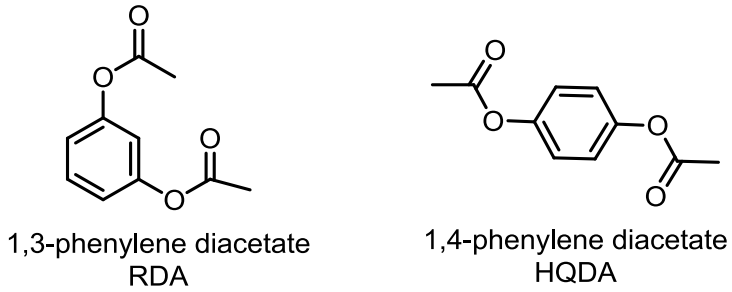

Figure 2.4: Chemical structures of RDA and HQDA

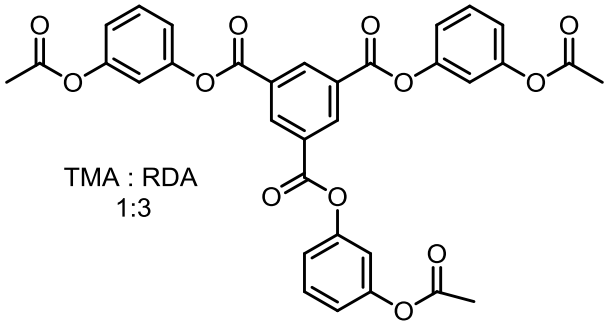

Figure 2.5: Chemical structure of TMA-RDA oligomer

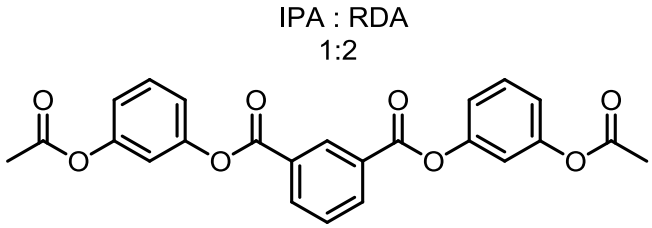

Figure 2.6: Chemical structure of RDA-IPA oligomer

2.2.2 Di-ABA Based Oligomers

3, 5-diacetoxybenzoic acid (Di-ABA) was chosen to substitute 1, 3, 5-benzene-tricarboxylic acid (trimesic acid, TMA). TMA has the highest melting point >300 ^{o}C among the above mentioned aromatic monomers since it has a strong H-bonding between molecules. The hydrogen atom bonded to the oxygen atom (–O–CO–) is electro-

statistically attached to another oxygen atom in another TMA molecule and thus it requires more energy to break the interaction. To weaken H bonding, the aprotic acetoxy ended functional group, which has no such H atom, is preferred to the carboxylic acid group. Di-ABA has a significantly lower melting point at 160 ^{o}C. Using Di-ABA instead of TMA could reduce the reaction time and temperature, while maintaining the ratio of crosslinker in the oligomer system. The monomer ratio of Di-ABA based oligomers is listed in the Table 2.1 and Table 2.2.

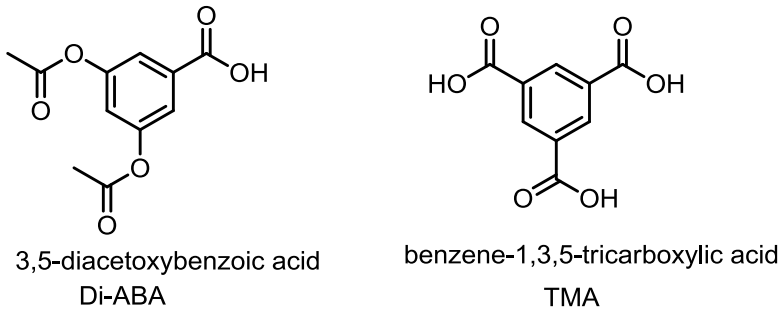

Figure 2.7: Chemical structures of Di-ABA and TMA

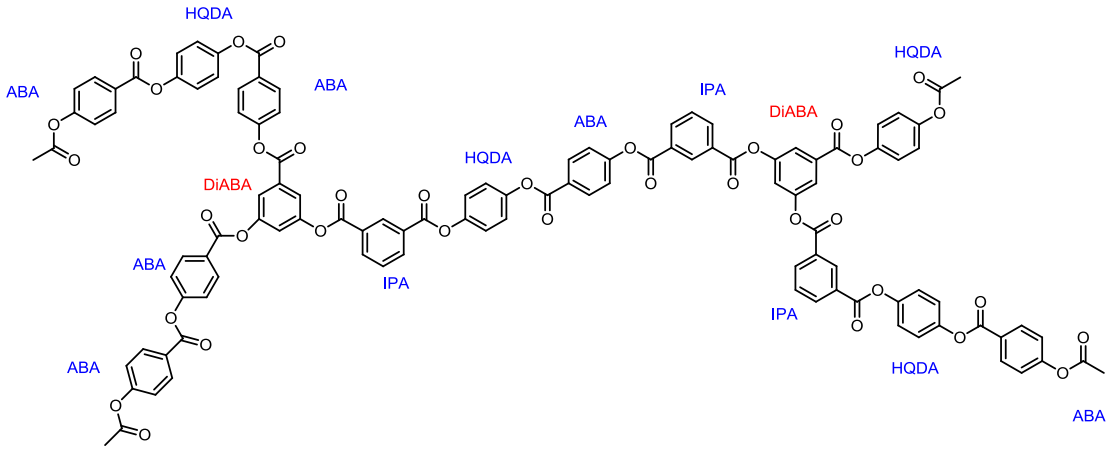

Figure 2.8: Schematic chemical structure of Di-ABA-acetoxy end oligomer

Table 2.1: Reactant ratio of Di-ABA-acetoxy end oligomer

Monomer	Molar Ratio	Carboxylic Acid	Acetoxy
Di-ABA	2	2	4
ABA	6	6	6
HQDA	4	-	8
IPA	3	6	-
Net	-	14	18

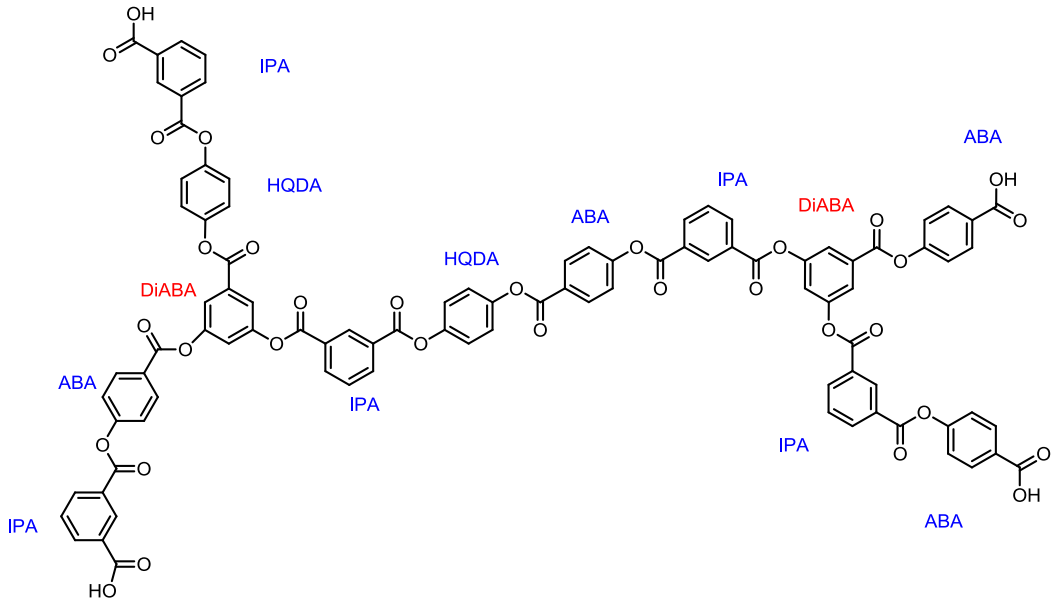

Figure 2.9: Schematic chemical structure of Di-ABA-carboxylic acid end oligomer

Table 2.2: Reactant ratio of Di-ABA-carboxylic acid end oligomer

Monomer	Molar Ratio	Carboxylic Acid	Acetoxy
Di-ABA	2	2	4
ABA	4	4	4
HQDA	2	-	4
IPA	5	10	-
Net	-	16	12

2.3 Characterization of ATSP Oligomers and Discussion

2.3.1 RDA Based Oligomers

Viscosity Test

Because 0.2 to 0.4 g/ml solution is commonly used for ATSP/fiber composites fabrication, 0.3g/ml oligomer/NMP solution is chosen for the viscosity test at 20 ^{o}C room temperature. Rotational centipoise viscometer, model #98936 was used. After immersing the spindle of viscometer into the oligomer solution, spinning mode was turned on and thus the viscometer starts to read the relative viscosity of the solution by measuring the torque required to turn the spindle.

Figure 2.10: Viscometer

Figure 2.11: Spindles

Table 2.3: Viscosity of oligomers

Oligomer	A1	A2	C1	RDA-IPA	RDA-TMA
Viscosity/ centipoise	40	60	180	0	10

Liquid Crystallinity

Cured ATSP polymer synthesized from certain oligomers exhibit liquid crystallinity since the rigid rod chains could form an organized three dimensional ordered network. It has been proved by the optical microscopy of ATSP/carbon fiber thin film sample. Birefringence is observed only around the surface of fiber in ATSP1 sample (cured product from A1-C1 oligomers) due to the local orientation of resin along the fiber direction, while isotropic behavior is observed in other regions. ATSP2 (cured product from A2-C2) forms an integral ordered liquid crystalline phase throughout the resin by comparison. [9, 19, 20]

Liquid Crystallinity is also observed after curing the RDA-based oligomers. Two samples are synthesized: RDA-TMA oligomer with C1 and RDA-IPA oligomer with C2. The solution of oligomers is dripped onto the flat glass slide and then heated to 270 ^{o}C overnight. The cured thin film is observed under transmission microscopy.

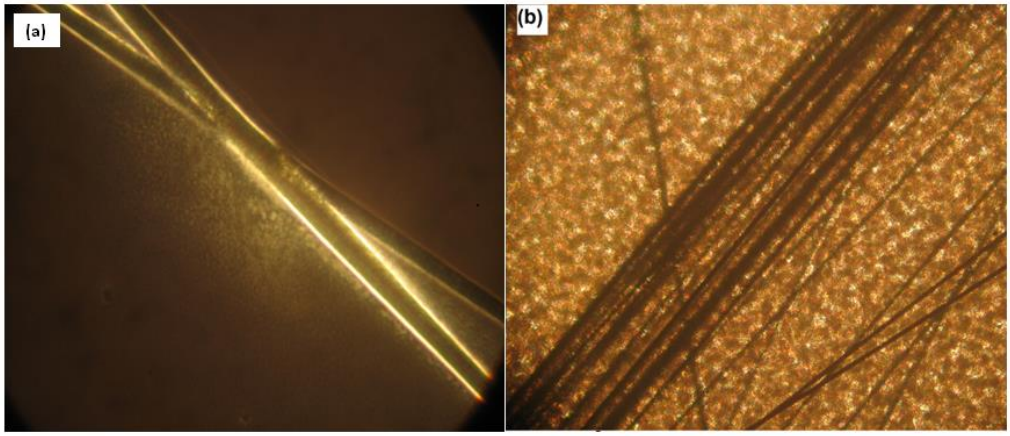

Figure 2.12: (a) ATSP1/carbon fiber; (b) ATSP2/carbon fiber.

From Dr. Parkar PhD thesis

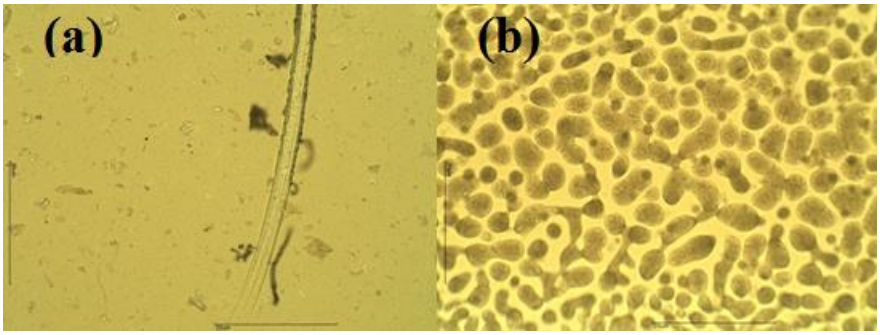

Figure 2.13: (a) RDA-TMA oligomer with C1; (b) RDA-IPA oligomer with C2

According to the optical microscopy result, RDA-IPA oligomer with C2 exhibits liquid crystallinity while the RDA-TMA oligomer with C1 doesn't. It might be the result of the structure difference between C1 and C2. C1 oligomer is more linear-like than C2. It's more difficult for it to form ordered phase due to the freedom of the chain. Another observation from the result is that, the dimension of crystal domain in RDA-IPA oligomer with C2 is not uniform, which might be the result of uneven film.

2.3.2 Di-ABA Based Oligomers

Measure of Molecular Weight

NMR spectroscopy is a widely used technique for characterizing chemicals. One of its well established applications is to determine the molecular weight of organic compounds. There are several methods to measure the molecular weight, including membrane osmometry, light scattering photometry, viscometry and gel permeation chromatography. Compared to the listed methods, NMR spectroscopy is a simple and rapid approach. Sample prepared for the test is Di-ABA-carboxylic acid end oligomer and C2. The schematic structures of these materials are provided in chapter 2.1 and chapter 2.2. Oligomer is dissolved in deuterated solvent inside a 5mm tube and measured in the UI400 ^{1}H-NMR spectrometer. The spectrum is analyzed by Mestrelab Software.

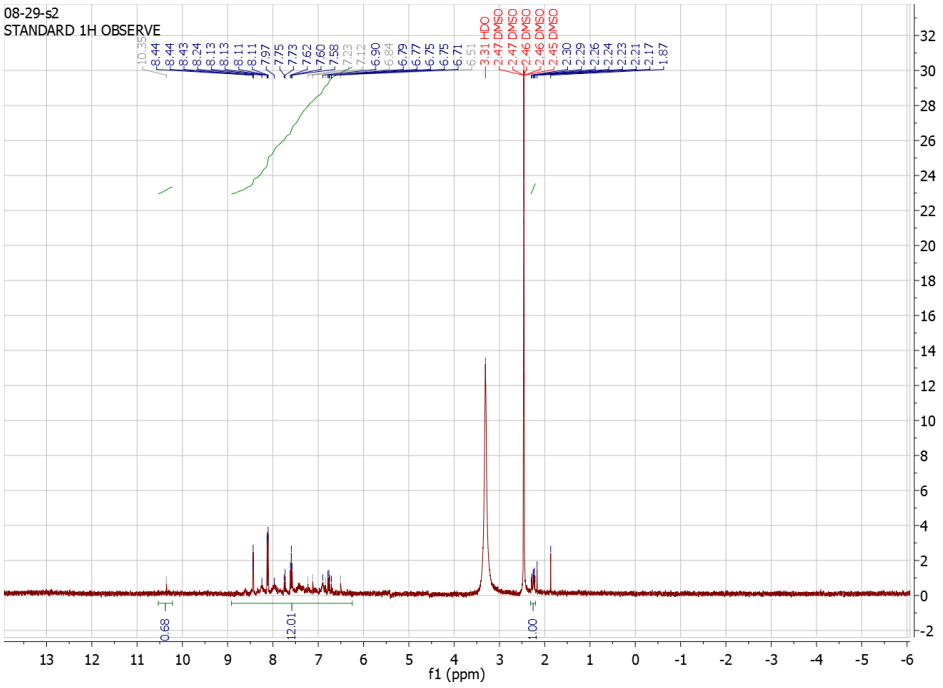

Figure 2.14: H^{1}-NMR of Di-ABA-carboxylic acid end oligomer

From the monomer ratio, Di-ABA: ABA: HQDA: IPA is 2: 4: 2: 5 and the corresponding molecular weights are 238, 180, 194, 166 g/mol. There are a total 36 of H atoms on acetoxy functional group in the blend of monomer. If the extent of the condensation reaction goes to 1, there are 50 H atoms on the benzene backbone of the

oligomer and the number of H atoms on acetoxy group is 3 ×unreacted units. 12 units of byproduct acetic acid are created and its molecular weight is 60 g/mol.

According to the spectra, the ratio of peak area H(6.50ppm-8.50ppm) to peak area H(2.21ppm- 2.30ppm) equals 12. H(6.50ppm-8.50ppm) represents the phenyl-H; and H(2.21ppm- 2.30ppm) represents the acetyl-H. By simple mathematics,

$$\text{Unreacted Unit} = \frac{50}{3} \times \frac{1}{12} = 1.39$$

Assuming that the Di-ABA, which acts as the crosslinker in the oligomer has fully reacted. The unreacted unit comes from ABA, HQDA or IPA.

$$\text{Average MW of Monomer (no crosslinker)} = (4 \times 180 + 2 \times 194 + 5 \times 166)/(4 + 2 + 5) = 176.2\ \text{g/mol}$$

$$\text{Acetic Acid} = 60 \times (12 - 1.39) = 636.6\ \text{g}$$

$$\text{MW of Di-ABA-carboxylic acid end oligomer} = 2 \times 238 + 4 \times 180 + 2 \times 194 + 5 \times 166 - 1.39 \times 176.2 - 636.6 = 1531\text{g/mol}$$

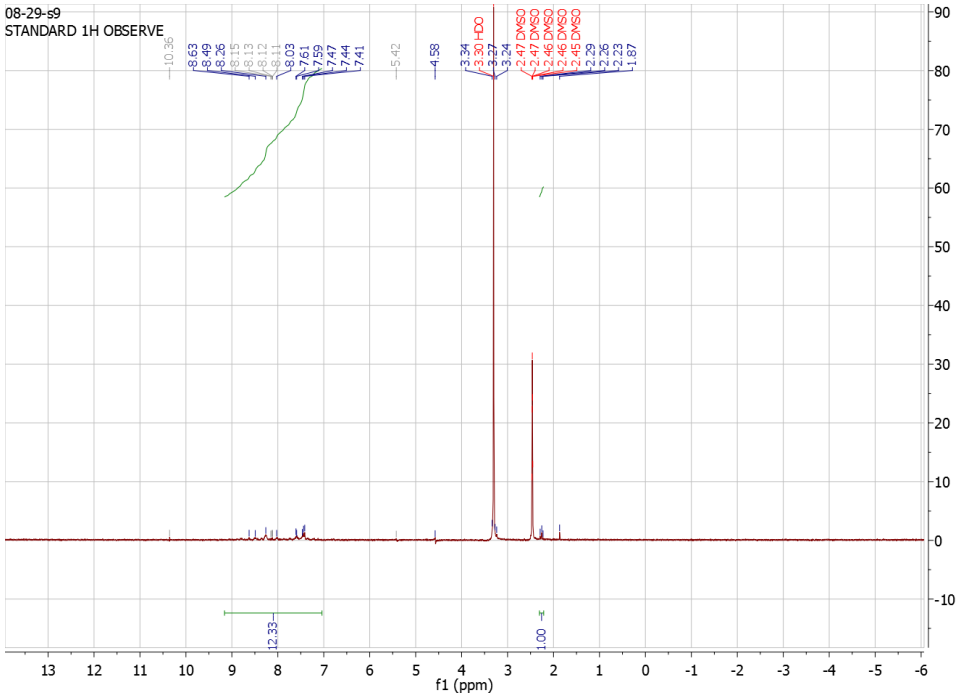

Figure 2.15: H^1-NMR of C2 oligomer

Similarly, the molecular weight of C2 oligomer is calculated from the H^1-NMR spectra.

$$\frac{\mathrm{H(phenyl)}}{\mathrm{H(acetyl)}} = \frac{59}{3 \times \text{unreacted unit}} = 12.33$$

$$\text{Unreacted Unit} = \frac{59}{3} \times \frac{1}{12.33} = 1.59$$

$$\text{MW of C2} = 6 \times 180 + 4 \times 194 + 4 \times 166 + 1 \times 210 - 1.59 \times 180 - 744.6 = 1699\ \mathrm{g/mol}$$

Each batch of oligomers can be tested by H^1-NMR and the molecular weight can be calculated in order to determine the extent of oligomer condensation reaction. As a result, the molecular weight of produced oligomers can be easily revealed.

2.3.3 Thermal Stability of ATSP Oligomers and Cured Resin

Thermogravimetric analysis (TGA) has been used to measure the thermal stability of chemicals. It records the weight difference of the sample during the heating process and therefore can tell the vaporization, sublimation and degradation of the chemicals. A series of oligomers, cured ATSP resins and commercially available high performance resins are tested.

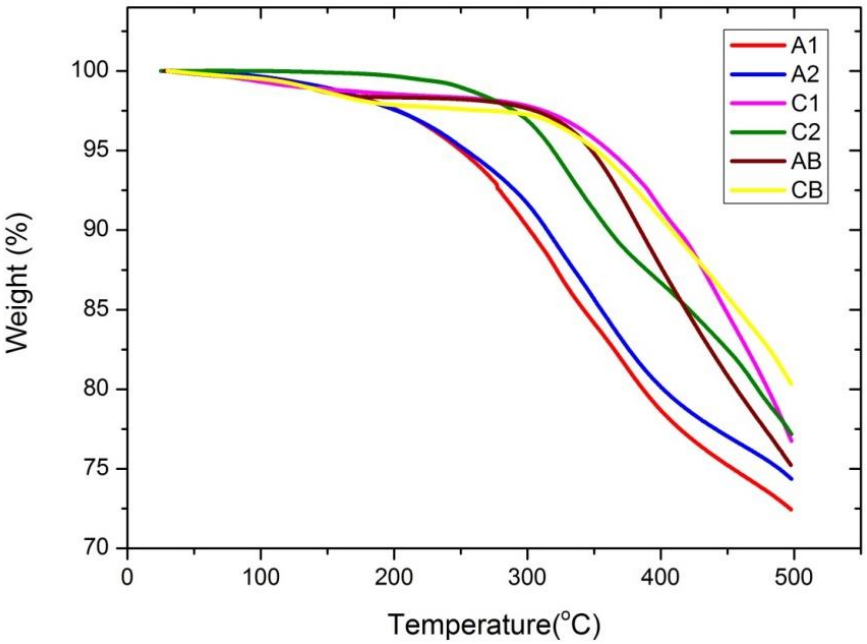

Figure 2.16: TGA analysis of oligomers

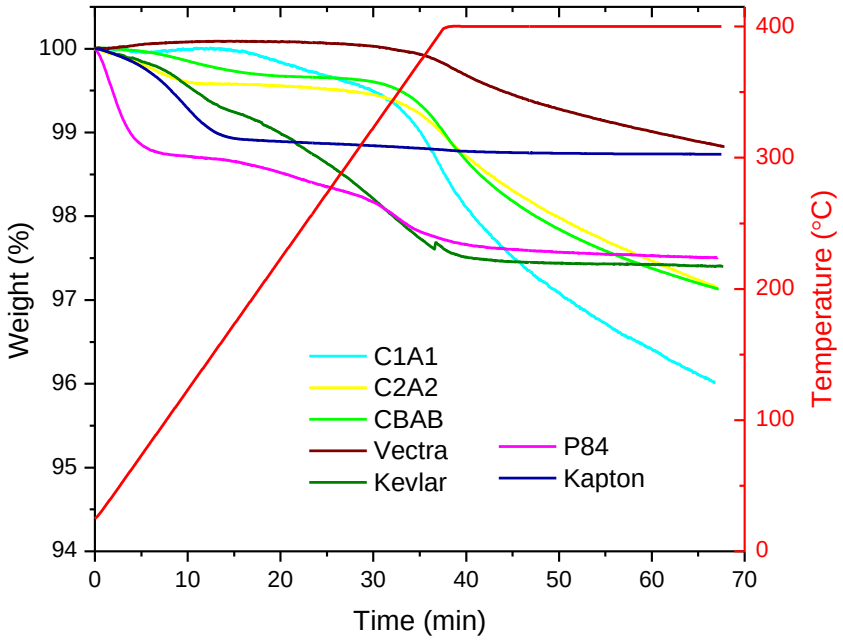

Figure 2.17: TGA analysis of cured resins, held at 400 ^{o}C for 30 minutes

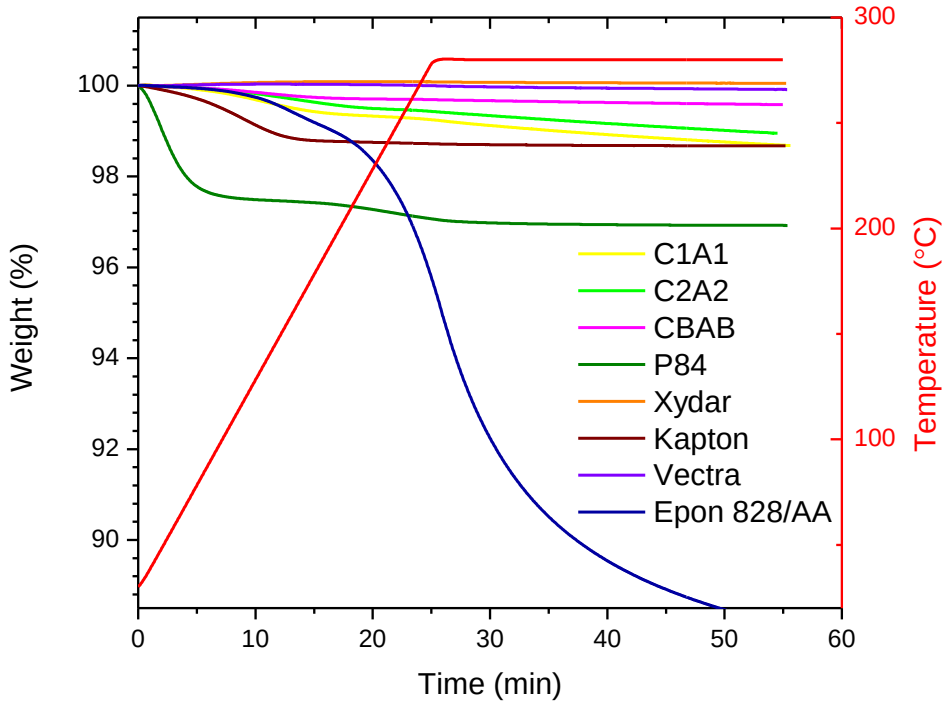

Figure 2.18: TGA analysis of cured resins, held at 280 ^{o}C for 30 minutes.

The TGA analysis indicates that cured ATSP resin could resist an aggressive high temperature. The thermal stability is comparable to commercially employed linear polymers such as Xydar, Kapton and Vectra. With the wide range of service temperature and resistance to high temperature, ATSP could be a high value and high performance thermoset resin.

2.4 Conclusion and Future Work

A set of low melting point oligomers are successfully synthesized by tailoring the composition of monomers. RDA and Di-ABA are chosen because of their low melting point and thus easy processability. The idea of selecting new monomers is based on the

understanding of stereochemistry and molecular structures. The structure and functionality of oligomers is tailored by the ratio of reactant monomers. Attempts of using RDA and Di-ABA based oligomers to synthesize ATSP didn't proceed smoothly as these oligomers could not be blended with other components well. However, they shows relatively low viscosity.

Various characterizations have been done to learn the viscosity, liquid crystallinity, thermal stability of ATSP oligomers and the resin. ATSP resin has outstanding thermal stability, which makes it possible for ATSP to be listed as another high performance material. Moreover, H^1-NMR has been proved to be an effective method to measure the molecular weight and to qualify the quality of each oligomer batch.

Future work could focus on developing possible oligomers based on easy handled monomers, such as RDA and Di-ABA, in order to enrich the family of ATSP. Studying the degradation of cured ATSP resin and the chemical behaviors occurred during the heating process should be considered too. This can help in providing more specific environment limit for the application of ATSP.

CHAPTER 3

STUDY OF ATSP/GLASS FIBER COMPOSITES AND ITS APPLICATION IN PRINTED CIRCUIT BOARD

3.1 Backgrounds

Fiber reinforced polymer composites are materials made of the polymer resin as the continuous matrix phase and the fiber as dispersed and stiff phase. The polymer matrix protects the fiber from corrosive chemicals and abrasion, while the fiber provides the mechanical load. Fiber reinforced polymer composites are one of the leading circuit board materials with high stiffness and high strength.

ATSP with high thermal stability, flame resistance and low coefficient of thermal expansion (CTE) can be employed as the matrix for printed circuit boards. Study of ATSP/carbon fiber which includes fiber induced liquid crystallinity of ATSP, flammability and mechanical properties of ATSP/carbon fiber and healing of interlaminar cracks by ITR reaction has been done by Dr. Parkar. Inspired by her work, ATSP/glass fiber has been prepared and tested. It opens the opportunity for developing a thermal stable circuit board laminate for high frequency electronic devices. [9]

Printed circuit board manufacturing technology was invented in 1930s. The circuit board is durable and compact and the electronic components can be easily soldered to the board. Epoxy/glass fiber laminate is a good combination of processability, performance and acceptable cost and it has been the commonly available circuit board substrate for years. As the working frequency of electronic devices increases nowadays,

low dielectric constant and good thermally conductive laminates need to be developed. In addition, resins with low CTE are required to avoid the thermal fatigue of the laminate. [21]

3.2 Fabrication of ATSP/Glass Fiber Composites

ATSP/glass fiber composite laminate were made from C1-A1 or C2-A2 oligomer solutions with glass fiber. For example, C1-A1 oligomer powders were dissolved in NMP to make the 50 wt% solution under mild heat by water bath. The viscosity of the solution was determined by the ratio of oligomer blends. Woven glass fiber mat was cut to 4×4 inch. Gently poured the flowing oligomer solution onto the glass fiber mat and pressed the solution by rolling glass rod in order to speed the filtration. Let the glass fiber mat stay in the oven at 50 ^{o}C overnight until the NMP evaporated. Then the ATSP/glass fiber prepregs were ready to be used.

The stack of prepregs underwent the curing process in the hot press at 100psi. The consolidation of ATSP oligomers and further ITR reaction enables the resin to bond to itself and the fiber glass thoroughly at 330 ^{o}C. The residual NMP solution and byproduct acetic acid evaporated after the curing. Therefore, the ATSP/glass fiber composite laminate was well prepared. Thick composite laminate were made by bonding individual laminates by ITR reaction. Copper foil was adhered to the surface of the laminate using ATSP oligomer solution as adhesive agent.

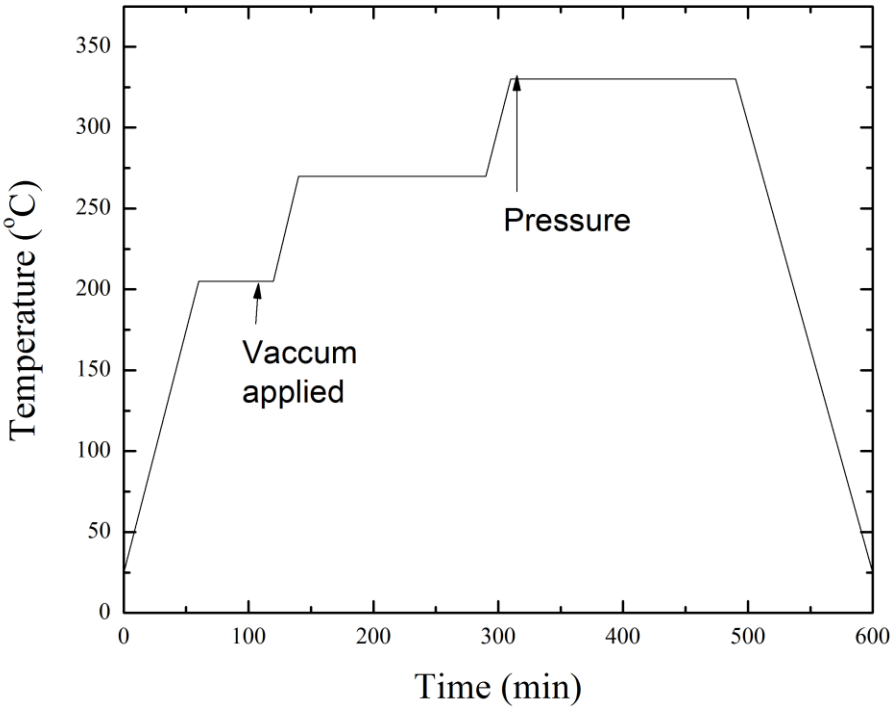

Figure 3.1: Cure cycle

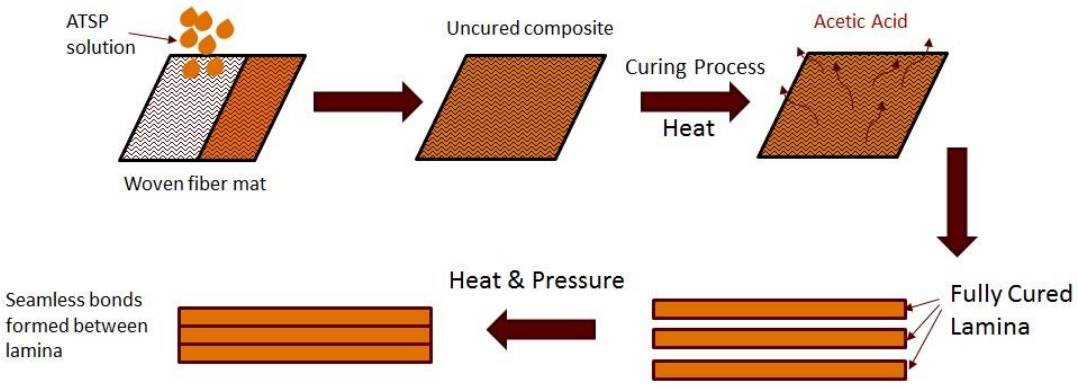

Figure 3.2: Schematic procedure of making ATSP/glass fiber laminate

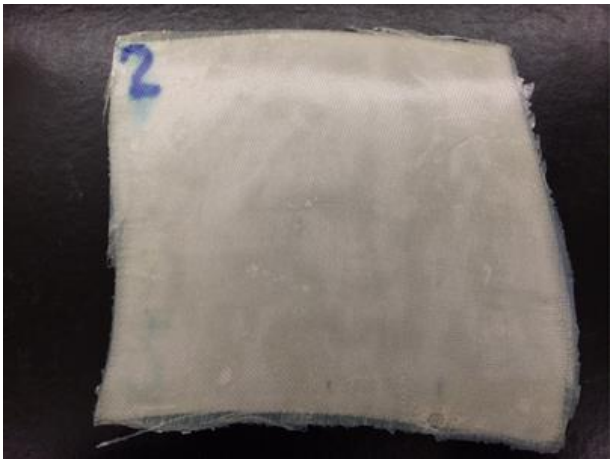

Figure 3.3: ATSP/glass fiber prepreg

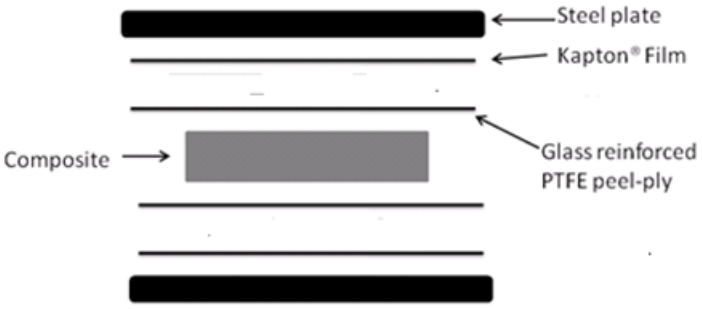

Figure 3.4: Schematic set up of laminate manufacture using hot press

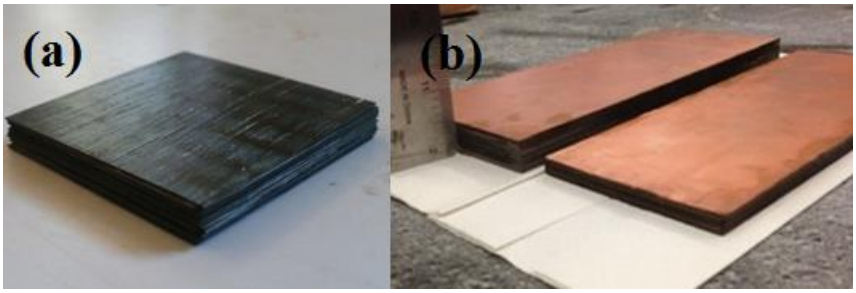

Figure 3.5: (a) ATSP/C laminate;

(b) ATSP/glass fiber laminates with copper foil

3.3 Mechanical Properties of ATSP/Glass Fiber Composites

3.3.1 Study of ATSP/Carbon Fiber Composites

According to the thesis of Dr. Pakar, ATSP/C composite shows better mechanical performance to epoxy/C composite. In addition, ATSP/C composite has a much lower transverse CTE, which means ATSP/C composites take only half of residual stress compared to that of Epoxy/C composite. As a result, ATSP/C composite could perform more stably over a range of temperature and the thermal fatigue of the laminate could be prevented. This assumption is proved by the thermal cycling experiment, during which ATSP/C composites has four times fewer microcracks compared to epoxy/C composite. The excellent reliable stability of the ATSP/C composites also comes from the fact that ITR reaction could repair the microcracks by exchanging the ester bonds and rearrange the three dimensional crosslinking networks. [14, 22]

Table 3.1: Tensile and shear properties of ATSP and Epoxy composites.

From Dr. Parkar PhD thesis

Property	Unit	ATSP/C V_{fiber}: 51.1%	Epoxy/C V_{fiber}: 70%
Young's Modulus	GPa	1.06 ±0.09	1.14 ±0.06
Young's Modulus Normalized (V_{fiber}: 55%)	GPa	1.141 ±0.096	0.896 ±0.05
Shear Modulus, G_{12}	GPa	8.27 ±0.83	7
Shear Strength, S_{12}	MPa	29.59 ±4.96	76

Table 3.2: CTE of ATSP and Epoxy composites

From Dr. Parkar PhD thesis

Property	Unit	ATSP/C V_{fiber}: 66.8%	Epoxy/C V_{fiber}: 72.4%
CTE, longitudinal	µm/^{o}C	-19.64	-21.69
CTE, transverse	µm/^{o}C	30.8	65.56

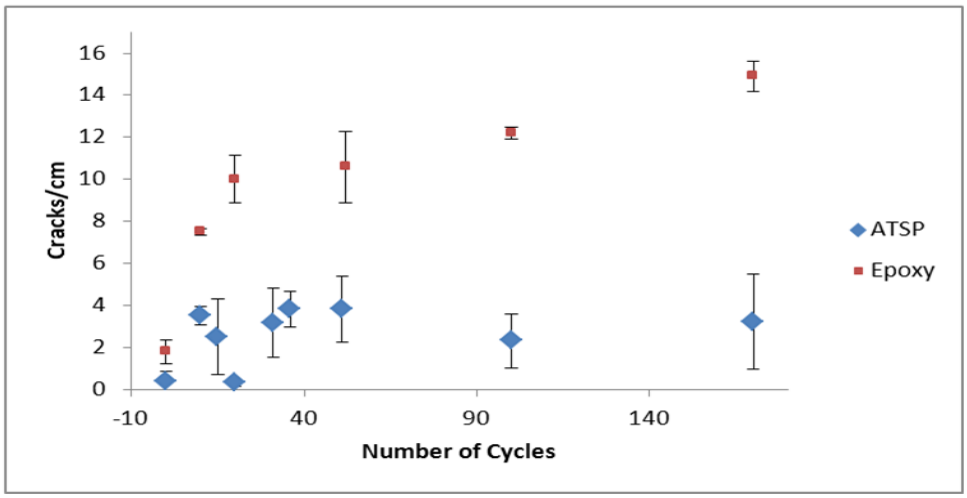

Figure 3.6: Number of microcracks on ATSP/C and Epoxy/C composites.

From Dr. Parkar PhD thesis

3.3.2 Interlaminar Shear Strength of ATSP/Glass Fiber Composites

The interfacial bonding between the relatively ductile polymer resin and the rigid fiber reinforcement is one of the primary issues for composites. Inadequate interlaminar bonding leads to delamination failure. Single fiber fragmentation test (SFFT) is a method to qualify the interface shear strength (ISS). In SFFT, a dogbone-shaped sample is strained to at least three times the elongation at failure of fiber it bears. The fragments of

fiber break into smaller pieces as the stress reaches the tensile strength and the process stops until the tensile stress at the fracture points reduce to zero. The fragment length of the fiber is then observed. The fragment lengths (l), fiber tensile strength (σ_f), and fiber diameter (d) are then related to the interfacial shear strength. [23]

$$\tau_i = K\frac{\sigma_f}{2}\left(\frac{d}{l}\right)$$

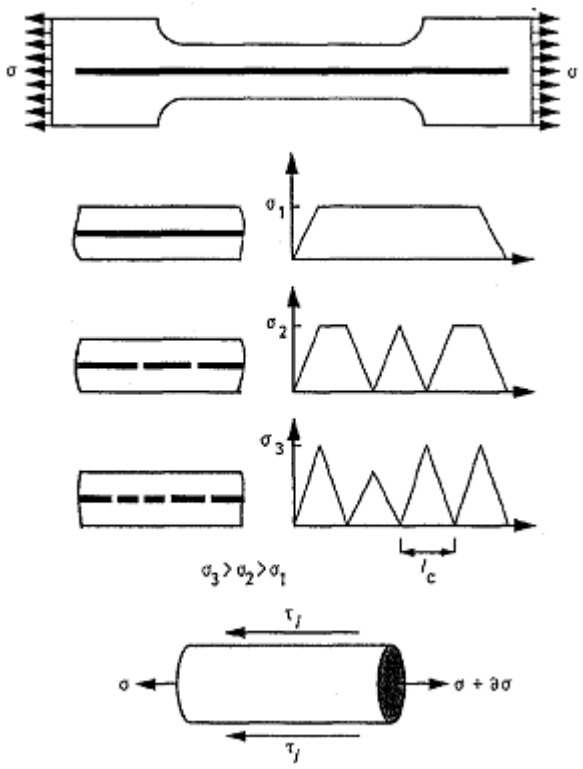

Figure 3.7: Schematic SFFT process

Experiment

Single filament of glass fiber and carbon fiber was separated from the tows and laid at the center of the dogbone-shaped PTFE mold individually. The ends of the fiber were secured by clay. ATSP oligomer solution was dripped upon the fiber surface as

coating. The mold was dried in the oven and then filled with the degased 31:32:32:37 mixtures of EPON 828, HELOXY 505, and Lindride 6K. The dogbone samples were cured at 120 ^{o}C for 4 hours.

The dogbone samples were tested in a micro-straining apparatus, which can apply sufficient load to fracture the sample. Fiber fragment lengths were measured under transmission microscope after the elongation reaches 20%.

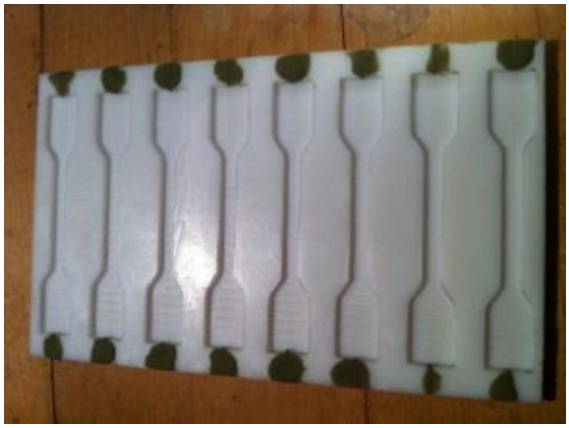

Figure 3.8: PTFE mold with single fiber lay up

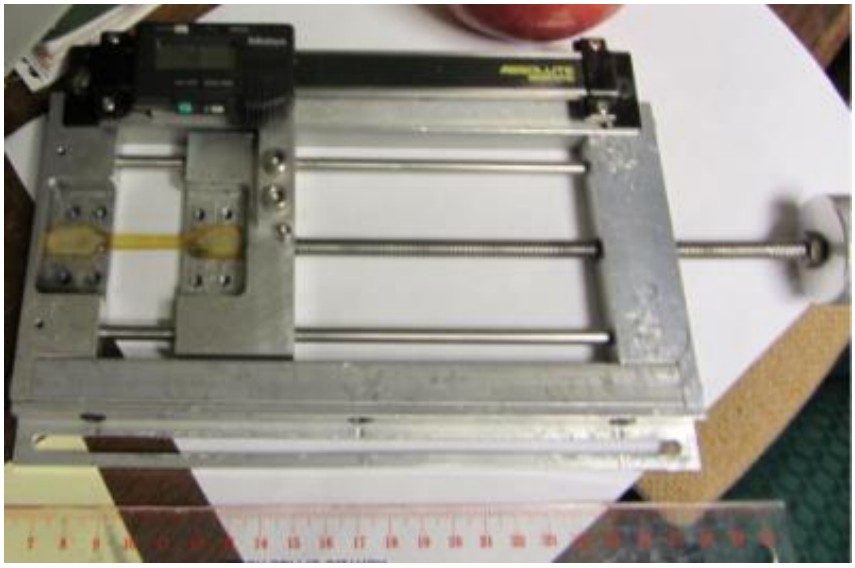

Figure 3.9: Micro-straining apparatus

Table 3.3: ISS of ATSP/glass fiber and ATSP/C composites

Interfacial Shear Strength	C1-A1 MPa	C2-A2 MPa
Glass fibers	63.9	72.8
Carbon fibers	53.5	84.2

Both ATSP1 and ATSP2 composite could match CTE at the resin-fiber interface, which helps reducing the residual stress and therefore a strong bonding is formed. The SEM picture of fracture indicates that the resin-fiber is mostly maintained, while there are tearing marking on resin. It proves that the interlaminar bonding is strong enough to resist the fracturing. [24]

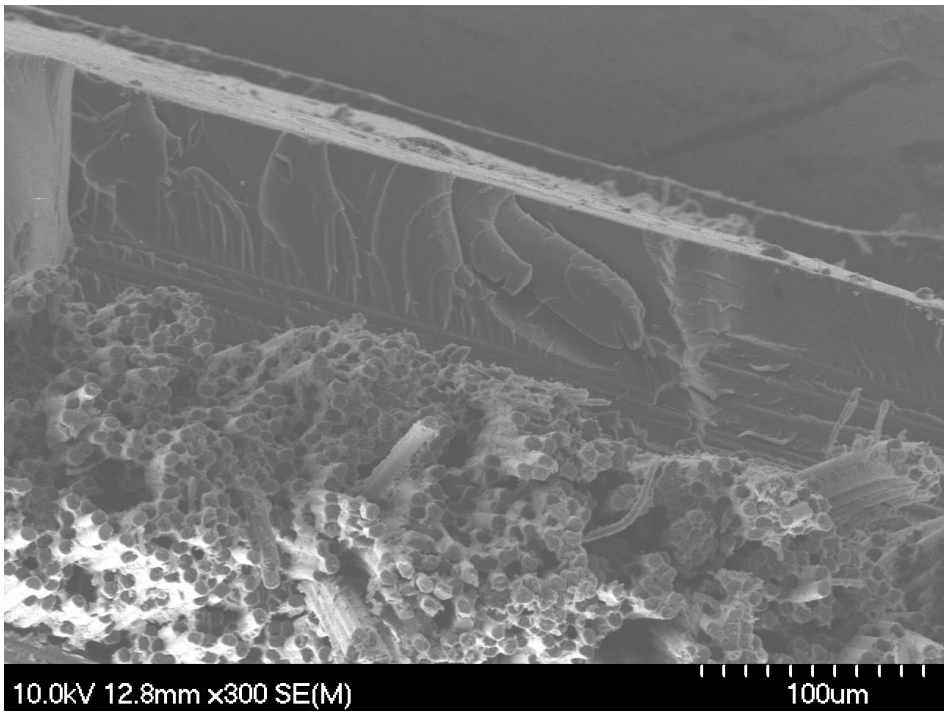

Figure 3.10: SEM of resin-fiber interface. From S. Bender Master thesis.

3.3.3 Scratch Test of ATSP/Glass Fiber Composites

Scratch test was performed on ATSP/glass fiber laminate. After cutting the surface by razor blade, the laminate went through the curing cycle. Pressure was added to bring in close contact around uneven scratch location. The surface of the laminate was tested by the Sloan Dektak^3 ST stylus surface profilometer before and after the curing cycle. The flatness of the surface clearly indicated that the scratch was partially healed by ITR reaction.

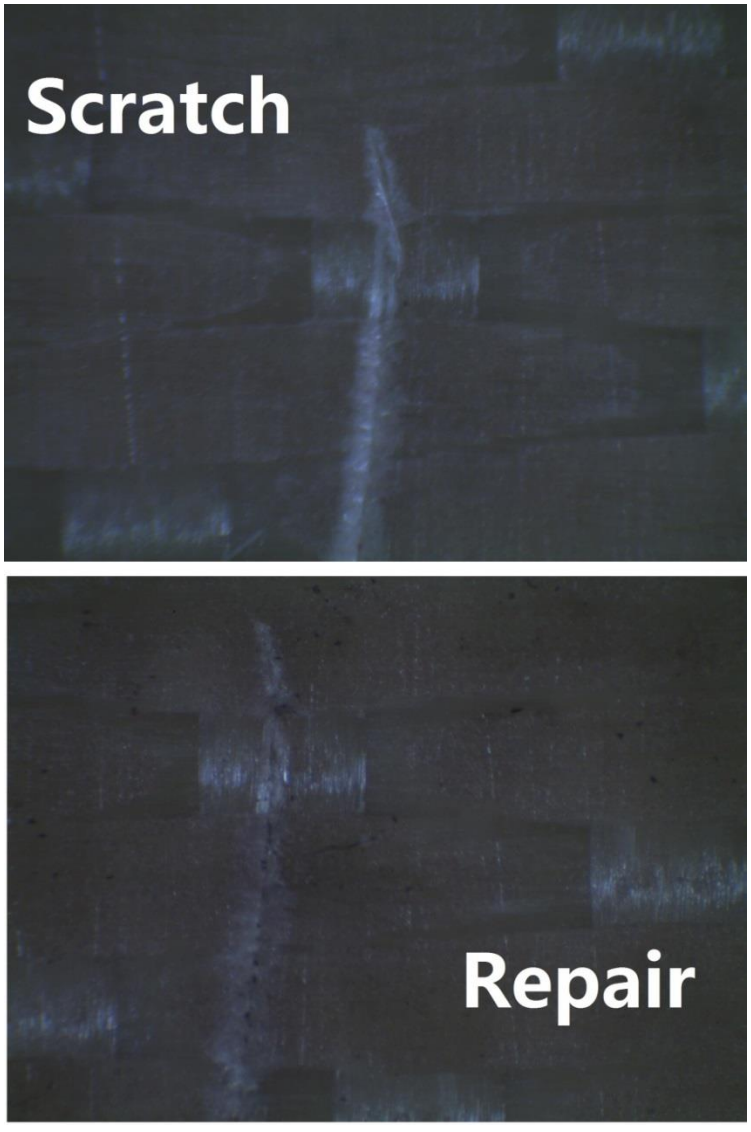

Figure 3.11: Surface of the laminate under transmission microscope

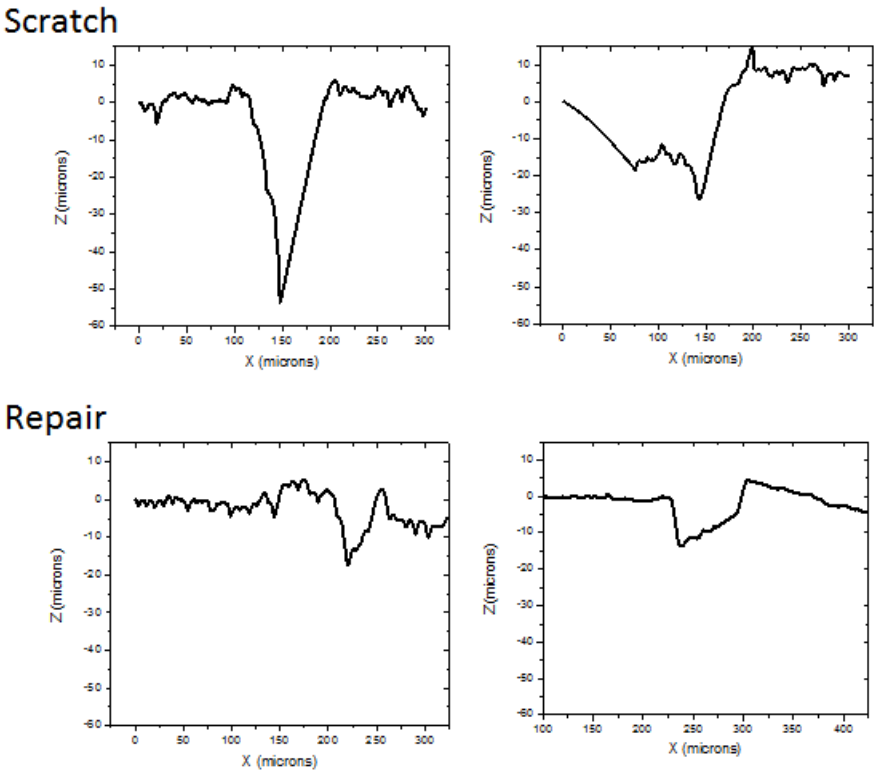

Figure 3.12: Surface flatness of ATSP/glass fiber laminate before and after ITR

3.4 Electrical Properties of ATSP/Glass Fiber Composites

ATSP/glass fiber composite laminate with plain copper trace was prepared and tested. The insertion loss at high frequency of ATSP/glass fiber is smaller than standard FR-4 substrate. The insertion loss is comprised of dielectric, conductor, leakage and radiation. It is a general term to describe the total loss of a radio frequency system. The experiment was done by Professor Jose E. Schutt-Aine's group at department of electrical and computer engineering.

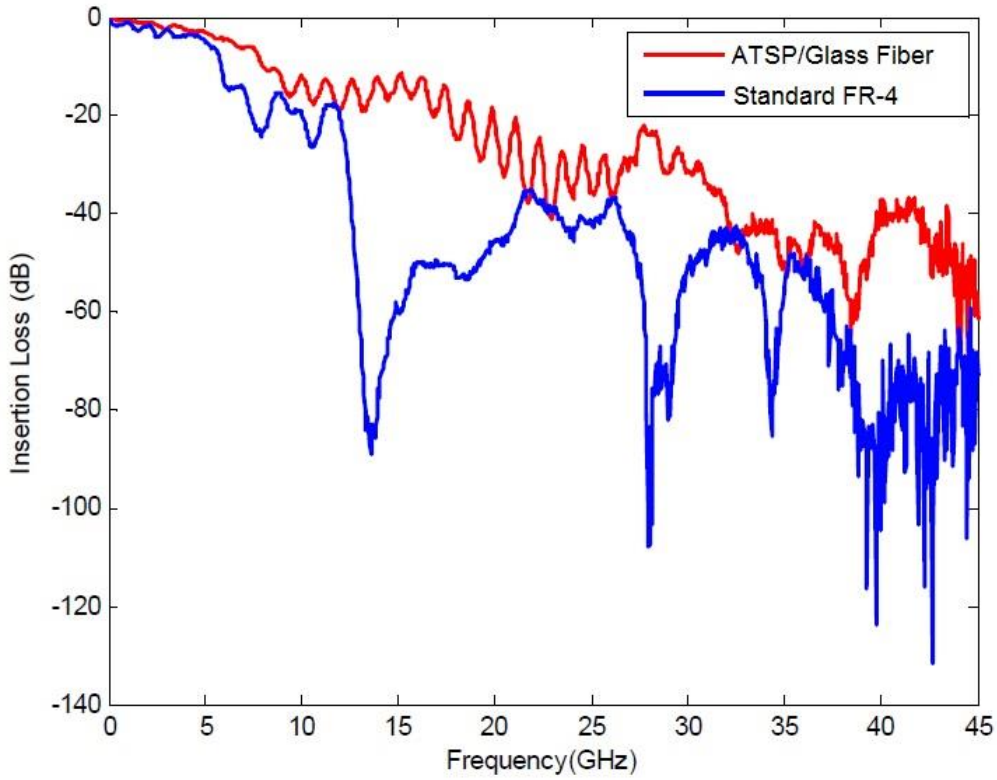

Figure 3.13: Insertion loss of ATSP/glass fiber laminate and FR-4

3.5 Conclusion and Future Work

ATSP/glass fiber composites have high thermal stability and water resistance. The fiber induced local orientation of ATSP benefits the interlaminar bonding between resin and fiber. Therefore, ATSP/glass fiber composites have excellent mechanical properties. ATSP can be tailored to obtain different morphologies, like C1-A1 copolyester and C2-A2 copolyester. The ITR reaction can repair the scratch surface of the laminate. Applications involving the healing of composites should be considered. Last but not least, the bonding between ATSP/glass fiber laminate and copper foil is waiting to be improved. Current copper-laminate adhesion has not been strong enough for complex etching process. Natural oxide on copper foil is difficult to be wetted by resin and has to

be washed off. Black copper oxide is introduced as oxidizing agent to modify the copper surface by strengthening the oxide layer and roughening the oxide surface. Both the formation of CuO during oxidization and the increased wettability of roughened copper surface can improve the peel strength. [25, 26]

REFERENCES

1. M. W. Jawitz, M. J. Jawitz, *Materials For Rigid And Flexible Printed Wiring Boards*, Taylor & Francis, 2006
2. Plastics International, *FR-4 Glass/Epoxy Phenolic data sheet*
3. F. Barontini, K. Marsanich, L. Petarca, V. Cozzani, *Ind. Eng. Chem, Res*, 44, 4186-4199 (2005)
4. G. Grause, M. Furusawa, A. Okuwaki, T. Yoshioka, *Chemosphere*, 71, 872–878 (2008)
5. Jan Azelson, *Making Printed Circuit Boards*, Tab Books, 1993
6. D. Frich, K. Goranov, L.Schneggenburger, J. Economy, Macromolecules, 29 (24), 734-7739 (1996)
7. S. G. Cottis, J. Economy, B. E. Nowak, *P-oxybenzoyl Copolyesters*, U.S. Patent, 3637595 A, Jan 25, 1972
8. S. G. Cottis, J. Economy, A. A. Wosilait, *Partially Crosslined Linear Aromatic Polyesters*, U.S. Patent, 3884876 A, Mar 20, 1975
9. Z. Parkar, PhD Thesis, University of Illinois, 2011
10. D. Frich, PhD Thesis, University of Illinois, 1991
11. K. Xu, PhD Thesis, University of Illinois, 1994
12. A. Lopez, J. Economy, *Polym Composites*, 22, 3 (2001)
13. L. A. Schneggenburger, P. Osenar, J. Economy, *Macromolecules*, 30, 3754-3758 (1997)
14. J. Zhang, PhD Thesis, University of Illinois, 2008
15. S. M. Yeo, PhD Thesis, University of Illinois, 2013

16. J. Economy, A. A. Polycarpou, J. Meyer, *Polymer Coating System for Improved Tribological Performance,* U.S. Patent, 20130337183 A1, Dec 19, 2013
17. J. Devaux, P. Godard, J. P. Mercier, R. Touillaux, J. M. Dereppe, *J. Polym. Sci. Pol. Phys.*, 20, 1881-1894 (1982)
18. E. Armelin, L. Franco, A. Rodriguez-Galan, J. Puiggali, *Macromol. Chem. Phys.*, 203, 1 (2002)
19. S. Beland, *High Performance Thermoplastic Resins and Their Composites*, 1991.
20. D. Frich, J. Economy, *J. Polym. Sci., Part A: Polym. Chem.*, 35 (6), 1061-1067.
21. K. C. Yung, B. L. Zhu, T. M. Yue, C. S. Xie, *J. Appl. Polym. Sci.*, 116, 518-527 (2010)
22. A. Lopez, J. Economy, *Polym. Compos.*, 22 (3), 444-449 (2001)
23. S. Feih, K. Wonsyld, D. Minzari, P. Westermann, H. Liholt, Riso-R-1483 (EN)
24. S. Bender, Master Thesis, University of Illinois, 2009
25. H. K. Yun, K. Cho, J. H. An, C. E. Park, *J. Mater. Sci.,* 27, 5811-5817 (1992)
26. K. Cho, E. C. Cho, J. *Adhesion Sci. Technol.,* 14 (11), 1333-1353 (2000)